Biophysical *Journal*
Biophysical Letter

Biophysical Society

Structure of Transmembrane Helix 8 and Possible Membrane Defects in CFTR

Valentina Corradi,[1] Ruo-Xu Gu,[1] Paola Vergani,[2] and D. Peter Tieleman[1,*]
[1]Centre for Molecular Simulation and Department of Biological Sciences, University of Calgary, Calgary, Alberta, Canada and [2]Research Department of Neuroscience, Physiology and Pharmacology, University College London, London, United Kingdom

ABSTRACT The cystic fibrosis transmembrane conductance regulator (CFTR) is an ion channel that regulates the flow of anions across epithelia. Mutations in CFTR cause cystic fibrosis. CFTR belongs to the ATP-binding cassette transporter superfamily, and gating is controlled by phosphorylation and ATP binding and hydrolysis. Recently obtained ATP-free and ATP-bound structures of zebrafish CFTR revealed an unwound segment of transmembrane helix (TM) 8, which appears to be a unique feature of CFTR not present in other ATP-binding cassette transporter structures. Here, using μs-long molecular dynamics simulations, we investigate the interactions formed by this TM8 segment with nearby helices in both ATP-free and ATP-bound states. We highlight ATP-dependent interactions as well as the structural role of TM8 in maintaining the functional architecture of the pore via interactions common to both the ATP-bound and ATP-free state. The results of the molecular dynamics simulations are discussed in the context of the gating mechanism of CFTR.

The cystic fibrosis transmembrane conductance regulator (CFTR) regulates anion flow through the apical membrane of epithelia (1). Defects in CFTR cause cystic fibrosis, a disease in which the movement of ions and water across epithelia is compromised, allowing for thick secretions to accumulate mainly in the airways, digestive, and reproductive systems (2). CFTR, although a member of the ATP-binding cassette transporter superfamily, functions as a channel, switching between closed and open states (3).

An interesting feature of several recently obtained CFTR structures is a region of transmembrane helix (TM) 8 that is partially unwound (residues 929–938 in zebrafish CFTR (zCFTR), corresponding to residues 921–930 in human CFTR (hCFTR)), thus breaking the α-helical structure (4–6). This feature, common to the ATP-free and ATP-bound states, might underlie CFTR's unique channel function (6). To investigate the interactions between this segment and nearby helices and how this segment can be partially unwound despite being in the membrane, we embedded the structure of zCFTR in the ATP-free and ATP-bound state in a 1-palmitoyl-2-oleoyl-sn-glycero-3-phosphocholine lipid bilayer. We performed atomistic molecular dynamics simulations for a total of 3 and 1.5 μs of simulation time for the ATP-free and ATP-bound systems, respectively (Fig. 1; Table S1).

The conformation of individual domains (transmembrane domains (TMDs) and nucleotide binding domains (NBDs)), based on root mean-square deviation, interdomain distances, and secondary structure analyses, remains stable over the simulations (Figs. S1–S4). In the ATP-free system, we noticed a closing motion of the NBDs, as has also been reported by others (7) (Fig. S1).

The unwound segment of TM8 remains stable during all the simulations in both systems (Figs. S3 and S4). The extracellular end of TM8, because of its different orientations in the ATP-free and the ATP-bound states (6), can establish interactions with residues of TM6 only in the presence of ATP (Y925-S342 (TM6)) (Fig. 2, *A* and *C*). If the hydrogen-bond interaction between this residue pair is not present in the ATP-bound state (Fig. 2 *C*), the distance between the α-carbons is not significantly increased (Fig. S5 *A*), with no noteworthy opening of the pore and the side chain of Y925 still facing the central pore (Fig. S5 *B*). The interaction between Y927 and S875 (TM8) is also detected only in the ATP-bound state (Fig. 2 *C*). Further along TM8, we identify several residues that interact with nearby helices in both states, i.e., the E932-R348 (TM6), S933-F312 (TM5), M937-Y305 (TM5), M937-Q1004 (TM9), and R941-E871 (TM7) pairs (Fig. S6). The ATP-free state of the hCFTR structure (4) adopts the same conformation as the ATP-free zebrafish one (5), and the residue pairs here analyzed for the zCFTR are conserved in hCFTR (Fig. 2 *D*; Table S2).

The unfolded segment of TM8 exposes the backbone and side chain of residues 930–941 to the hydrophobic region of

Submitted November 14, 2017, and accepted for publication March 5, 2018.
*Correspondence: tieleman@ucalgary.ca
Editor: Jose Faraldo-Gomez.
https://doi.org/10.1016/j.bpj.2018.03.003

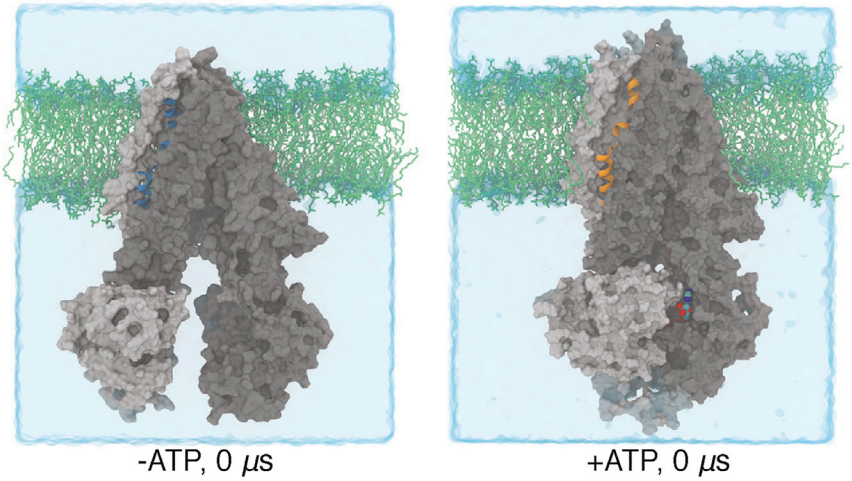

FIGURE 1 Simulation setup. The ATP-free (−ATP, *left*) and ATP-bound (+ATP, *right*) zCFTR structures were embedded in a 1-palmitoyl-2-oleoyl-sn-glycero-3-phosphocholine bilayer (*light green sticks*). TMD1-NBD1 and TMD2-NBD2 are shown in dark and light surfaces, respectively. TM8 is highlighted in blue and orange cartoons for the two systems. Water (*light cyan surface*) and lipids are clipped for clarity.

the lipid bilayer, with the side chain of R941 reaching E871 (TM7) to establish salt-bridge interactions (Fig. 2, *A*, *E*, and *F*). In the ATP-free state, we observed simulations in which the salt bridge between these two residues is missing, leading to the penetration of water and lipid headgroups inside the membrane and the formation of a clear water channel (Fig. 2 *E*; Fig. S7). This membrane defect, once established, remains stable for the duration of the simulation. Water molecules from the main cavity of the channel can also contribute to the pool of water molecules. In the absence of the defect, water molecules from the inner cavity of CFTR can reach this region of TM8 to interact with E871 and R941. Y927 participates in these interactions only in the ATP-free state (Fig. 2, *E–G*).

In all other ATP-binding cassette exporter structures, the TMs are organized in a roughly symmetrical pattern with no breaks in their helical structure (8). The unwound segment of TM8 is then a unique feature of CFTR (4–6) that suggests a solution for a long-standing puzzle: why are the transmembrane helices known to line the permeation pathway not symmetrically distributed between TMD1 and TMD2? In particular, cysteine-accessibility studies performed on TM7 and TM1 gave very different results (9–11), indicating that the latter, but not the former, formed part of the permeation pathway (12,13). Chen and colleagues (4–6) discovered that the unwound portion of TM8 and the resulting bend position the extracellular end of TM8 closer to the permeation pathway. This displaces TM7 further from the protein's central axis, thus explaining the lack of contribution of TM7 to the anion permeation pathway.

Contacts between TM8 and TM6 are known to be required for maintaining the functional architecture of the channel, as in the case of residues E932 and R348 (14,15), the interaction of which is retrieved in both ATP-bound and ATP-free simulation systems (Fig. S6). TM8 also interacts with TM5, from the intracellular side to the kink at F312, allowing dynamic interactions that stabilize the unwound segment of TM8 in both simulation systems. Overall, although not many of the residues that form molecular contacts with the unwound stretch of TM8 have been studied functionally, the network of molecular contacts between TM8 and the nearby helices investigated in our simulations can explain the stability of the unwound segment in both the ATP-free and the ATP-bound state and is consistent with an active role of TM8 in the functional structure of the channel.

However, the current ATP-bound structure is not a fully open channel, and the protrusion of TM8 residues toward the central pore interferes with anion flow, confirmed by the fact that an interaction is formed between TM8 and TM6, located in the narrowest portion of the pore (3,16). Thus, within the gating cycle of CFTR, the ATP-dependent interaction between the N-terminal of TM8 and TM6 might be transient as part of an intermediate state that provides an additional gate preventing anion flow through the channel. Although ATP binding and NBD dimerization are coupled with the channel entering the "open burst" state (17), "flicker" closures of the pore occur within the open burst with timescales that are not consistent with ATP hydrolysis (18–20). As suggested by Zhang and colleagues (6), the ATP-bound cryo-electron microscopy structure might have captured a flicker-closed state artifactually stabilized by experimental conditions. The alternative hypothesis proposed by these authors, that the extracellular TM8 (and TM12) might reorientate within microseconds to a position allowing fast anion flow, seems unlikely, given the relatively stable position of these secondary structure elements and the lack of a major opening of the pore between TM8 and TM6.

Two of the ATP-free, inward-facing simulations showed an unusual lipid organization near TM8. A strong membrane defect forms near R941 and E871, whereas no lipid headgroups were found in the proximity of these residues in the remaining three ATP-free simulations or in the two ATP-bound ones. Although the presence of charged residues buried along TM helices is not common, there are examples in which such residues play important biological roles, for instance, in integrin receptors (21). The presence of a

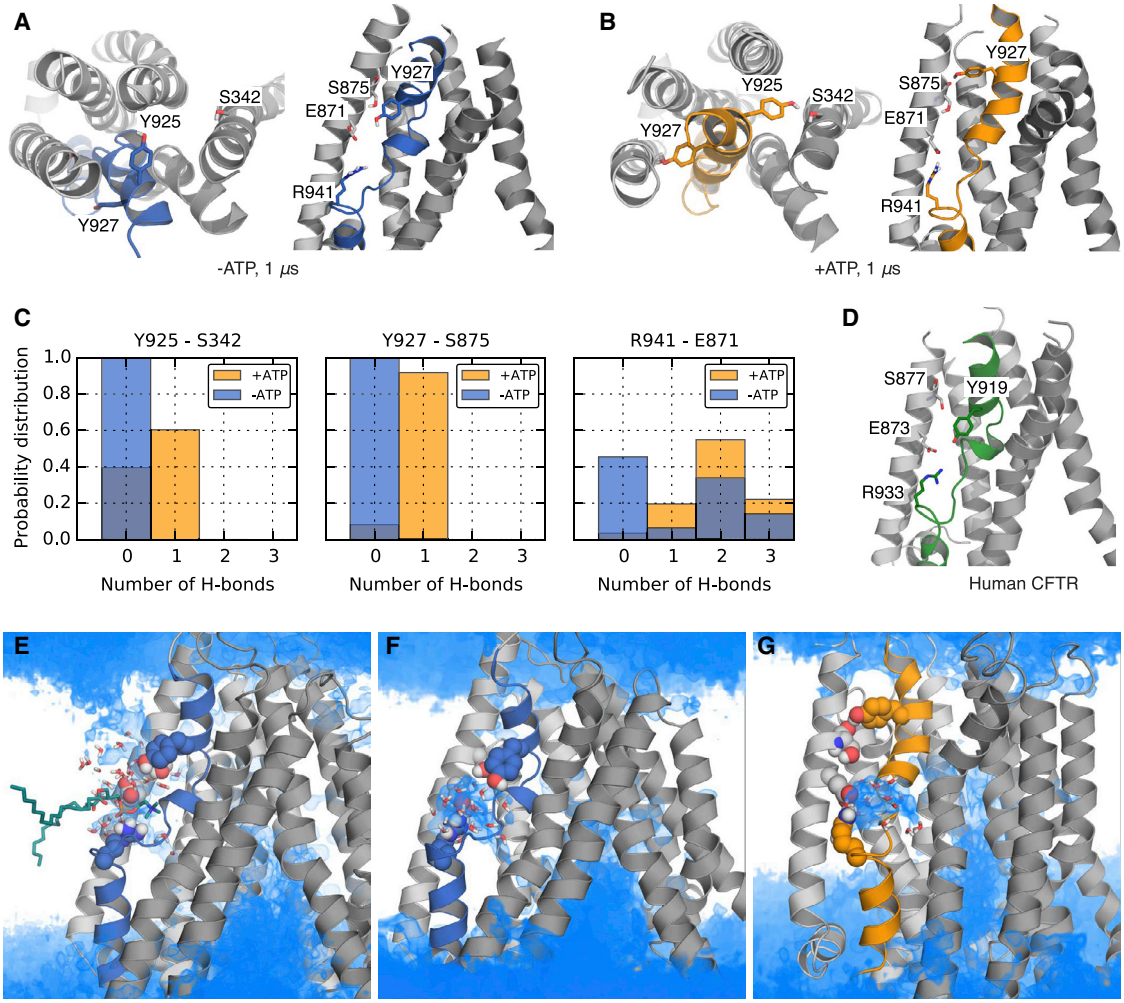

FIGURE 2 TM8 orientation and selected interactions. (*A* and *B*) Extracellular and side views of TM8 and neighboring helices in the ATP-free (−ATP) and ATP-bound (+ATP) system after 1 μs of simulation time are shown. The side chains of residues Y925, S342, Y927, S875, R941, and E871 are shown as sticks. TMD1 and TMD2 are shown in dark and light gray cartoons, respectively, with TM8 highlighted in blue (−ATP) and orange (+ATP) cartoons. (*C*) The probability distribution of the number of hydrogen bonds detected between the selected residue pairs is shown in blue for the ATP-free simulations (−ATP) and in orange for the ATP-bound (+ATP) simulations. (*D*) Side view of TM8 (*green*) in the ATP-free, hCFTR structure (Protein Data Bank: 5UAK). The residues corresponding to the zebrafish residues shown in panels (*A*–*C*) are shown as sticks. (*E*–*G*) The number density of water molecules, calculated during the last 50 ns of the simulation, is shown as a blue volume map and overlapped to the last frame of (*E*) the 1-μs-long ATP-free simulation, showing the membrane defect; (*F*) run 3 of the ATP-free, 500-ns-long simulation, with no membrane defect; and (*G*) the 1-μs-long ATP-bound simulation, with no membrane defect. The protein is represented as in panels (*A* and *B*). The side chains of Y927, S875, E871, and R941 are shown as spheres, and the nearby water molecules within an 8-Å cutoff from R941 and E871 are shown as sticks. A lipid molecule with the headgroup interacting with R941 is shown in dark teal sticks (*E*).

membrane defect with lipid headgroups and water molecules located in the bilayer middle is associated with a substantial energetic cost, although this cost can be compensated for by a sufficiently hydrophobic sequence in the TM (22–24). R941 and E871 engage in stable salt-bridge interactions that can screen the charges from the hydrophobic environment of the lipid tails, requiring no headgroups to be pulled in to interact with R941. However, when stable interactions are not formed, this screening effect does not take place, and thus the membrane defect and the cone of water molecules compensate for the charges of R941 and E871. One reason for this defect forming only in the ATP-free state could be a more polar environment surrounding E871 and R941 in the absence of ATP: here, the extracellular end of TM8 not only orients away from the central pore, but also partially rotates (with respect to the ATP-bound state) so that the side chain of Y927 points toward the hydrophobic region of the bilayer (Fig. 2; Fig. S8). This allows the Y927 side chain to interact with water molecules and lipid headgroups once the defect is formed (Fig. 2, *E* and *F*). In the ATP-bound system, on the other hand, the simulations show a persistent interaction between Y927 and S875, with Y927 prevented from interacting with water molecules, together with a more buried R941 side chain (Figs. 2 and

S8). It should be noted that the cryo-electron microscopy structures of CFTR do not provide detailed density for the side chain of E871, and thus structural artifacts due to a nonideal initial side-chain modeling can occur. However, for each ATP-free and ATP-bound simulation, we carried out independent equilibration steps to allow for the sampling of different side-chain conformations. Thus, it seems plausible that a membrane defect, although a rare event, might occur in the ATP-free state, linked to a more polar environment because of Y927 and a more exposed R941 side chain.

Combined, our simulations support the stability of the unusual unwound segment of TM8 in the ATP-bound and ATP-free state of CFTR. The simulations also highlight a pool of interactions, common to both states, between TM8 and nearby helices that prevent further folding or unfolding of TM8 and contribute to the architecture of the channel. Although at present we can only speculate on the specific role of the residues we investigated, this study supports the development of experimental hypotheses to evaluate the contribution of TM8 residues, and in particular R941 interactions with other TMs and/or lipid headgroups, to the gating mechanism of CFTR.

SUPPORTING MATERIAL

Supporting Materials and Methods, eight figures, two tables, and three data files are available at http://www.biophysj.org/biophysj/supplemental/S0006-3495(18)30300-X.

AUTHOR CONTRIBUTIONS

V.C., P.V., and D.P.T. designed the project. R.-X.G. performed the simulations and carried out the DSSP analysis. V.C. performed the remaining analyses and wrote the manuscript with P.V. and D.P.T, with contributions from R.-X.G.

ACKNOWLEDGMENTS

We would like to thank Jue Chen, Rockefeller University, for helpful information on cryo-EM density maps.

This work was supported by the Canadian Institutes of Health Research. Additional support came from Alberta Innovates Health Solutions and Alberta Innovates Technology Futures. R.-X.G. is supported by fellowships from Alberta Innovates Health Solutions and the Canadian Institutes for Health Research (funding reference number: MFE-140949). D.P.T. holds the Alberta Innovates Technology Futures Strategic Chair in (Bio)Molecular Simulation. Simulations were run on Compute Canada machines, supported by the Canada Foundation for Innovation and partners. This work was undertaken, in part, thanks to funding from the Canada Research Chairs program. P.V. thanks the Cystic Fibrosis Trust for support.

REFERENCES

1. Rommens, J. M., M. C. Iannuzzi, …, N. Hidaka. 1989. Identification of the cystic fibrosis gene: chromosome walking and jumping. *Science.* 245:1059–1065.
2. Cheng, S. H., R. J. Gregory, …, A. E. Smith. 1990. Defective intracellular transport and processing of CFTR is the molecular basis of most cystic fibrosis. *Cell.* 63:827–834.
3. Linsdell, P. 2017. Architecture and functional properties of the CFTR channel pore. *Cell. Mol. Life Sci.* 74:67–83.
4. Liu, F., Z. Zhang, L., …, J. Chen. 2017. Molecular structure of the human CFTR ion channel. *Cell.* 169:85–95.e8.
5. Zhang, Z., and J. Chen. 2016. Atomic structure of the cystic fibrosis transmembrane conductance regulator. *Cell.* 167:1586–1597.e9.
6. Zhang, Z., F. Liu, and J. Chen. 2017. Conformational changes of CFTR upon phosphorylation and ATP binding. *Cell.* 170:483–491.e8.
7. Tordai, H., I. Leveles, and T. Hegedűs. 2017. Molecular dynamics of the cryo-EM CFTR structure. *Biochem. Biophys. Res. Commun.* 491:986–993.
8. Locher, K. P. 2016. Mechanistic diversity in ATP-binding cassette (ABC) transporters. *Nat. Struct. Mol. Biol.* 23:487–493.
9. Wang, W., Y. El Hiani, …, P. Linsdell. 2014. Relative contribution of different transmembrane segments to the CFTR chloride channel pore. *Pflugers Arch.* 466:477–490.
10. Gao, X., Y. Bai, and T. C. Hwang. 2013. Cysteine scanning of CFTR's first transmembrane segment reveals its plausible roles in gating and permeation. *Biophys. J.* 104:786–797.
11. Wang, W., Y. El Hiani, and P. Linsdell. 2011. Alignment of transmembrane regions in the cystic fibrosis transmembrane conductance regulator chloride channel pore. *J. Gen. Physiol.* 138:165–178.
12. Linsdell, P. 2014. Functional architecture of the CFTR chloride channel. *Mol. Membr. Biol.* 31:1–16.
13. Zhang, J., and T. C. Hwang. 2015. The fifth transmembrane segment of cystic fibrosis transmembrane conductance regulator contributes to its anion permeation pathway. *Biochemistry.* 54:3839–3850.
14. Cotten, J. F., and M. J. Welsh. 1999. Cystic fibrosis-associated mutations at arginine 347 alter the pore architecture of CFTR. Evidence for disruption of a salt bridge. *J. Biol. Chem.* 274:5429–5435.
15. Cui, G., C. S. Freeman, …, N. A. McCarty. 2013. Two salt bridges differentially contribute to the maintenance of cystic fibrosis transmembrane conductance regulator (CFTR) channel function. *J. Biol. Chem.* 288:20758–20767.
16. Gao, X., and T. C. Hwang. 2015. Localizing a gate in CFTR. *Proc. Natl. Acad. Sci. USA.* 112:2461–2466.
17. Vergani, P., S. W. Lockless, …, D. C. Gadsby. 2005. CFTR channel opening by ATP-driven tight dimerization of its nucleotide-binding domains. *Nature.* 433:876–880.
18. Zhou, Z., S. Hu, and T. C. Hwang. 2002. Probing an open CFTR pore with organic anion blockers. *J. Gen. Physiol.* 120:647–662.
19. Aleksandrov, A. A., L. Aleksandrov, and J. R. Riordan. 2002. Nucleoside triphosphate pentose ring impact on CFTR gating and hydrolysis. *FEBS Lett.* 518:183–188.
20. Vergani, P., A. C. Nairn, and D. C. Gadsby. 2003. On the mechanism of MgATP-dependent gating of CFTR Cl- channels. *J. Gen. Physiol.* 121:17–36.
21. Kim, C., T. Schmidt, …, M. H. Ginsberg. 2011. Basic amino-acid side chains regulate transmembrane integrin signalling. *Nature.* 481:209–213.
22. Ulmschneider, M. B., J. P. Ulmschneider, …, S. H. White. 2017. Transmembrane helices containing a charged arginine are thermodynamically stable. *Eur. Biophys. J.* 46:627–637.
23. Dorairaj, S., and T. W. Allen. 2007. On the thermodynamic stability of a charged arginine side chain in a transmembrane helix. *Proc. Natl. Acad. Sci. USA.* 104:4943–4948.
24. MacCallum, J. L., W. F. Bennett, and D. P. Tieleman. 2008. Distribution of amino acids in a lipid bilayer from computer simulations. *Biophys. J.* 94:3393–3404.